Simulation of spatial constant velocity transmission using equivalent RL approximation circuits

Pham Thanh Long*, Nguyen Ngoc Ha

Thai Nguyen University of Technology, No. 666, 3rd of February Street, Tich Luong, Thai Nguyen, Vietnam.
*Corresponding author: kalongkc@gmail.com
Received 6 Jun. 2026; Revised 14 Aug. 2026; Accepted 04 Sep. 2026; Published 16 Sep. 2026.
DOI: https://doi.org/10.54939/1859-1043.j.mst.FMC.2026.219-228

ABSTRACT

In engineering, numerous systems are either inaccessible or prohibitively expensive to evaluate using their original physical models. In such cases, equivalent models serve as viable alternatives. This approach requires a rigorous mathematical foundation to ensure that conclusions drawn from the equivalent model remain valid for the original system. From a modeling perspective, while machine learning (ML) models can approximate highly complex laws with significant precision, they often lack the ability to explain the underlying physical mechanisms, thus being categorized as "black boxes." The latest global trend in machine learning involves integrating physical relationships into model training (Physics-Informed Machine Learning). This integration offers dual benefits: the data-driven accuracy of ML and the interpretability of physical models. This paper presents the mathematical foundations for approximating the kinematic atlas of a mechanical object using an equivalent RL circuit as a surrogate model. Achieving high approximation accuracy enables the potential to represent various kinematic atlases through electrical circuits. This paves the way for circuit-based simulation research across diverse domains, combining both precision and the transparency of "grey-box" modeling. This methodology represents a highly promising research direction in modern engineering, offering a robust alternative to conventional black-box approaches.

Keywords: Machine Learning; Black box model; Physical transfer function; RLC Circuits; Kinematic atlases; Cardan.

1. INTRODUCTION

In modern engineering, the simulation and analysis of complex mechanical systems, particularly spatial constant velocity transmissions and parallel robots, require a rigorous balance between predictive accuracy and computational efficiency. Traditional research has long relied on analytical models or numerical methods such as the Finite Element Method (FEM); however, these approaches often face limitations when deployed in real-time applications or systems with large-scale spatial kinematic structures. Recently, the surge in Artificial Intelligence has introduced data-driven methodologies, yet pure machine learning (ML) models are frequently criticized as "black boxes" due to their lack of physical interpretability.

To address these shortcomings, a dominant paradigm shift is reshaping the scientific community: Physics-Informed Machine Learning. The foundational work by Raissi et al. [1] demonstrated that embedding partial differential equations (PDEs) directly into neural network architectures not only enhances accuracy with small datasets but also ensures that predictions consistently adhere to fundamental physical laws. This trend was further consolidated by comprehensive reviews on the potential of machine learning in the natural sciences [2], emphasizing the critical role of integrating prior physical knowledge with the computational power of big data. Additional research has explored data-driven predictive modeling using field inversion to enhance these frameworks [3].

Parallel to algorithmic advancements, a modeling approach based on systemic analogy is experiencing a resurgence. Utilizing equivalent electrical circuits to represent mechanical objects offers exceptionally fast simulation speeds by leveraging specialized solvers in electronic

engineering. Furthermore, it creates a transparent grey-box structure regarding energy flow. Port-Hamiltonian Systems theory [4] provides a robust mathematical framework for mapping multi-domain physical interactions into network structures, enabling the description of energy flow, storage, and dissipation through components analogous to resistors and inductors.

Building upon these premises, recent literature has applied equivalent circuit modeling to parallel robots for energy consumption estimation [5] and explored the Foster realization of the inerter concept for vehicle suspensions [6]. Modern advancements also include digital twins that integrate Jacobian maps with real-time physics engines [7] and comparative studies between deep learning and analytical models in predicting singularity-free workspaces [8]. The integration of Physics-Informed Neural Networks (PINN) for robot kinematics [9] and the standardized principles found in the Springer Handbook of Robotics [10] further validate this hybrid approach. Finally, methodologies such as fault diagnosis using impedance fingerprinting [11] and energy-optimal trajectory planning based on equivalent mechanical impedance [12] demonstrate the practical utility of the electrical domain in solving mechanical challenges.

This paper proposes a novel methodology: approximating the kinematic atlas [13] of a mechanical object using an equivalent RL circuit. Rather than employing abstract mathematical interpolation functions, we develop an approximation circuit capable of precisely describing spatial transmission relationships. This approach not only inherits the interpretability of physical models but also harnesses the flexible approximation capabilities inherent in machine learning. This represents a promising research direction for transitioning complex mechanical problems into the electrical domain, optimizing the simulation process while maintaining the physical transparency of the system.

2. PROBLEM

2.1. Theoretical foundations

2.1.1. Problem Statement

A common scenario in engineering practice involves a research object that has already been mathematically modeled. It is assumed that from this model, the input (I) – output (O) relationship can be discretized into two fields reflecting the characteristic properties of the original model. In practice, there are no constraints on the nature of these initial fields; they may be entirely stochastic depending on the specific research context. The relationship between field (I) and field (O) is described by a mapping (W), which serves as the original function as shown in (1):

$$I.\mathrm{W} = O \tag{1}$$

In cases where the original function has not yet been established, and experimental data only provides measurements of the two fields (I) and (O) without W, it becomes necessary to create an RL circuit entity with a dual role:

- Interpolation function: Bridging the discrete points of (I) and (O), similar to the existence of function W;

- Explanatory function: Elucidating the intrinsic nature of W, a task that machine learning is unable to perform.

There is a distinct difference between the original object (W), the machine learning (ML) function, and the surrogate function (RL circuit). Specifically, taking the original function (W) as the benchmark, machine learning only ensures the reproduction of interpolation relationships. This means (ML) only reflects accuracy within the scope of the known datasets (I) and (O). Conversely, because the surrogate model (RL circuit) is a physical model, its substitution remains valid for both interpolation and extrapolation. Due to this inherent physical nature, the RL circuit surrogate model allows for the explanation of the (I) and (O) relationship based on energy, leveraging established conservation laws.

Currently, although research on replacing systems with continuous (I)/(O) properties is relatively common worldwide, solutions remain limited for highly nonlinear systems with only discrete data that require high precision.

2.1.2. Determine the equivalent circuit model

The relationships in the original atlas usually take the form:

$$Input\ (I) \rightarrow Original\ function \rightarrow Output\ (O) \quad (2)$$

This relationship is not physical; it only functions to copy input to output, purely mathematically. We need to find an alternative function that can explain the relationship of the original function based on the energy transformation occurring in the system.

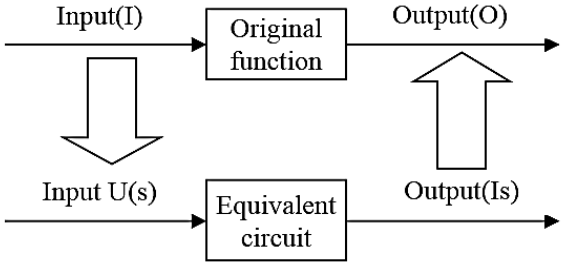


Figure 1. *Equivalent replacement model and input-output relationship.*

There are two mappings that need to be performed before finding the replacement function:

- The xyz transformation $\rightarrow$ U(s), this is a very complex mapping and is proposed according to the properties of each Atlas type, usually based on the energy/distance relationship, etc;

- The Output transformation between the two models is usually a linear mapping with a simple coefficient K, meaning the output only needs to follow the rule, the coefficient K adjusts the absolute position;

In short, before identifying the replacement function, its input and output rules have already been prepared using two arrays of real numbers corresponding to the input and output rules of the original function. To evaluate the fit of the two models, the difference in output data between the two models, evaluated by the R^2 coefficient, must be at a necessary level.

The proposed alternative model with Foster circuit, given the requirements for the interactions to be replicated during robot simulation in Section 2.1.1, constructs a general RL alternative circuit as follows.

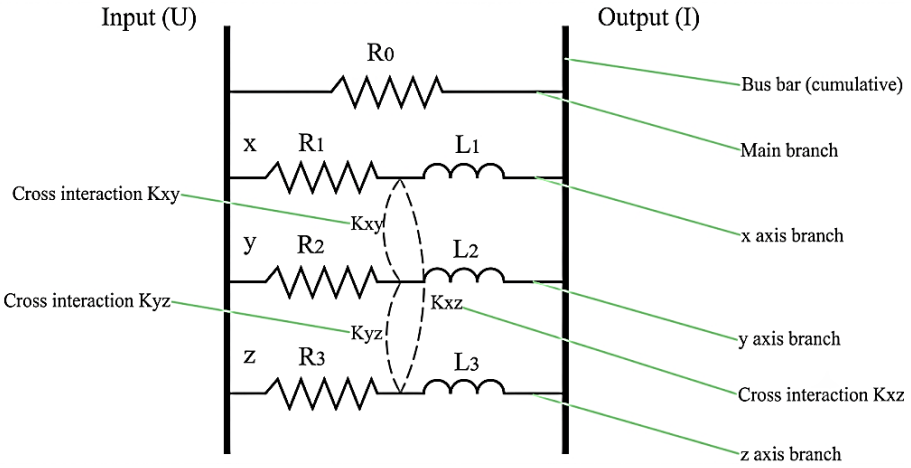


Figure 2. *Circuit diagram with explanation of the function of the elements.*

The expression for the output current is (without capacitor C):

$$I_{total}(s) = I_{R_0}(s) + \sum_{i=1}^{3} I_{Branch-i}(s) + \sum_{jk\in(xy,yz,xz)} I_{Branch-jk}(s) \quad (3)$$

Case with only RL circuit:

$$I_{total}(s) = \frac{U(s)}{R_0} + \sum_{i=1}^{3} \frac{U(s)}{L_i s + R_i} + \sum_{jk\in(xy,yz,xz)} \frac{K_{jk}.\Delta U_{jk}(s)}{T_{jk}s + 1} \quad (4)$$

The auxiliary branches, called Foster branches, have a similar structure, each consisting of 5 parameters:

- Resistance (R) defines the amplitude of (O), determining the strength of the transmitted signal in that direction;

- Inductance (L) defines the delay and inertia, which are parameters that cause internal noise in the branch;

- Capacitor (C) (if present in a high-order circuit) represents the energy storage capacity or periodic variations of the robot structure;

- Cut-off frequency or slope (ω, Q) defines the affected area of that branch in the workspace (the area this branch is sensitive in);

- Contribution factor (α weight) determines the percentage that this branch contributes to the total output current (O) compared to the other branches.

Table 1. *Circuit parameter statistics.*

Branch type	**Quantity**	**Total parameters**	**Main ingredients**	**Role in the NN network**
Main branch	1	5	R, L, C, ω, α	(O) base-level basic powertrain capabilities
Straight branch	3	15	R, L, C, ω, α	Learn the independent characteristics of each x, y, and z axis.
Cross branch	3	6	K,T	Learn about nonlinear interactions and mutual delays between pairs of axes.
Total	7	26		A unique encoder for each robot.

2.2. Introduction to the Cardan joint structure

2.2.1. Structural kinematics

Spatial constant velocity transmission is a type of transmission in which rotational motion is transferred from the input shaft to the output shaft with identical angular velocities at every moment, regardless of any spatial misalignment angle between the two shafts. In other words, if the input shaft rotates uniformly at an angular velocity ω, the output shaft will also rotate uniformly at that exact velocity, without any fluctuations or variations relative to the rotation angle. For example, in automotive steering systems, to link the steering wheel with the wheels, a Cardan joint (or universal joint) must be used to transfer motion and change direction in space, as illustrated in Figure 3.

A universal joint (also known as a U-joint or Cardan joint) is a coupling or joint that connects rigid shafts whose axes are inclined toward each other. It is commonly used in shafts that transmit rotational motion.



Figure 3. *Cardan shaft in the car's steering system.*

However, the Cardan joint suffers from a major drawback: even when the input drive shaft rotates at a constant speed, the output drive shaft rotates at a variable speed, thereby causing vibration and wear. The velocity fluctuation of the driven shaft depends on the joint's configuration, which is defined by three variables.

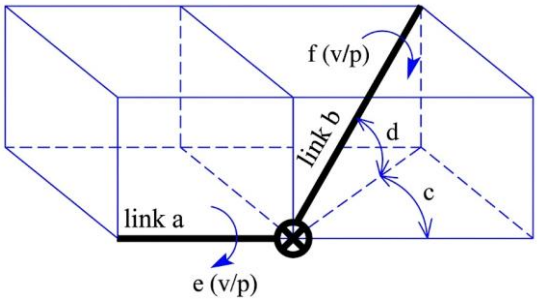


Figure 4. *Diagram of the variables of a universal joint.*

Figure 4 illustrates two half-shafts, a and b, of the transmission system connected via a Cardan joint. The two angles, c and d, represent the two direction cosines of half-shaft b relative to half-shaft a. The angular velocity of half-shaft a is constant and denoted as e, while the variable angular velocity of half-shaft b is denoted as f. These specific notations were chosen to facilitate ease of typing and drafting from a standard keyboard.

In practice, to avoid a self-locking condition where no amount of torque applied to half-shaft a can induce rotation in half-shaft b, the transmission misalignment angles c and d are typically restricted within the range of [-30º, +30º].

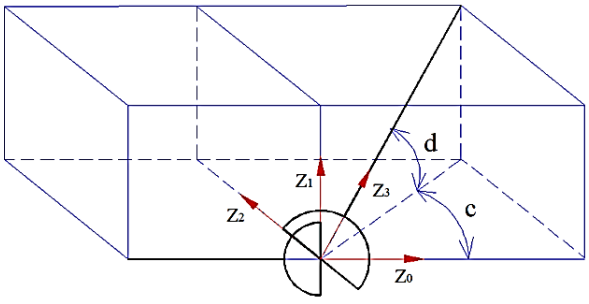


Figure 5. *The frames of reference are attached to the axes of rotation of the joint.*

Figure 5 illustrates the four rotational axes of the mechanism:

- Axis z_0: The rotational axis of half-shaft a, representing the input motion of the mechanism (the displacement magnitude is denoted by a constant e (rpm)).

- Axis z_1: The rotational axis around the cross-pin (spider) attached to half-shaft a.

- Axis z_2: The rotational axis around the cross-pin attached to half-shaft b.

- Axis z_3: The rotational axis of half-shaft b itself (its magnitude, denoted as f (rpm), varies depending on the position of the input shaft).

The fundamental rotation matrices are defined as follows:

$$rot(x,\alpha)=\begin{bmatrix}1 & 0 & 0\\ 0 & c\alpha & -s\alpha\\ 0 & s\alpha & c\alpha\end{bmatrix}; rot(y,\beta)=\begin{bmatrix}c\beta & 0 & s\beta\\ 0 & 1 & 0\\ -s\beta & 0 & c\beta\end{bmatrix}; rot(z,\gamma)=\begin{bmatrix}c\gamma & s\gamma & 0\\ -s\gamma & c\gamma & 0\\ 0 & 0 & 1\end{bmatrix} \quad (5)$$

Let β be the spatial angle between the two half-shafts a and b, and assume that x_0 is perpendicular to the plane containing both a and b. In the base reference frame, the input axis is defined as $\mathbf{z}_0 =(0,0,1)^T$. Since the output axis z_3 forms an angle β with the input axis, we have:

$$\mathbf{z}_3 = rot(x_0,-\beta)\cdot\mathbf{z}_0 = (0,\sin\beta,\cos\beta)^T \quad (6)$$

We want z_1 to be a unit vector lying in the x_0y_0 plane at an angle e relative to x_0. A concise way to construct it from z_0 is as follows:

$$\mathbf{z}_1 = rot(z_0,e)\cdot rot(y_0,+90^o)\cdot\mathbf{z}_0 = (\cos(e),\sin(e),0)^T \quad (7)$$

Construct z_2 from z_0 through a rotation sequence: first, rotate z_0 about x_0 by an angle β to transform z_0 into z_3 (as shown in Equation (6)); then, rotate about z_3 by an additional angle f, followed by a rotation about the y_3 axis by 90^o to correctly orient z_2 as described in Equation (8) below:

$$\begin{aligned}\mathbf{z}_2 &= Rot(x_1,-\beta)\cdot Rot(z_3,f+90^0)\cdot Rot(y_3,-90^0)\cdot\mathbf{z}_0\\ &= (\sin(f),-\cos(\beta)\cdot\cos(f),\sin(\beta)\cdot\cos(f))^T\end{aligned} \quad (8)$$

Since z_1 and z_2 are the two axes of the Cardan joint, they must be perpendicular to each other; therefore, their dot product must be zero ($\mathbf{z}_1.\mathbf{z}_2 = 0$). By substituting the corresponding coordinates calculated above, we obtain Equation (9):

$$\begin{aligned}&\mathbf{z}_1\cdot\mathbf{z}_2 = [\cos(e),\sin(e),0]\cdot[\sin(f),-\cos(\beta)\cdot\cos(f),\sin(\beta)\cdot\cos(f)] = 0\\ &\Leftrightarrow \cos(e)\cdot\sin(f) = \cos(\beta)\cdot\sin(e)\cdot\cos(f)\end{aligned} \quad (9)$$

For a standard phased joint (where the two yokes are coplanar), the relationship between the output angle (f) and the input angle (e) depends solely on the misalignment angle β, as illustrated in (10).

$$\tan(f) = \cos\beta\cdot\tan(e) \quad (10)$$

Calculate the solution, taking into account the signs of the corresponding quadrants:

$$f = \mathrm{a}\tan 2[\cos(\beta)\cdot\tan(e)] \quad (11)$$

The atan2 function is employed to uniquely determine the angular domain. The kinematics of the velocity transmission from e to f is expressed as follows. Set $\omega_a = e' = \frac{2\pi e}{60}(rad/s)$ Assuming the angular velocity of link a is constant (e = const), we take the derivative with respect to time as follows:

$$\frac{df}{de} = \frac{\cos\beta}{1-\sin^2\beta.\sin^2 e} \quad (12)$$

Therefore, the instantaneous velocity of link b is:

$$\omega_b(e) = f' = \omega_a \frac{\cos\beta}{1-\sin^2\beta.\sin^2 e} \tag{13}$$

Convert the units to revolutions per minute (rpm):

$$f(e) = e.\frac{\cos\beta}{1-\sin^2\beta.\sin^2 e}, \quad \beta = ar\cos(\cos c.\cos d) \tag{14}$$

The average velocity remains equal to e (as the Cardan joint maintains a constant average transmission ratio). However, f exhibits second-order fluctuations relative to e.

For small values of β :

$$f \approx e[1-\frac{1}{2}\tan^2\beta.\cos(2e)] \tag{15}$$

2.2.2. Constructing the discrete atlas description between Input (I) and Output (O)

Run the Cardan joint model (15) using the input shaft speed e (rpm) and the misalignment angle β . This generates a set of input-output relationships that need to be simulated via the equivalent circuit. This dataset is referred to as the training set (or sample set), a snippet of which is presented in Figure 7.

Explanation of data columns in Figure 7, parameter definitions and simulation objectives the parameters presented in the dataset are defined as follows:

- c^o, d^o: Direction cosines of half-shaft b relative to half-shaft a;

- e (rpm): Rotational speed of the driving shaft (input speed);

- β : The spatial misalignment angle between the two half-shafts, derived from c and d;

- f_{min}, f_{max}, f_{avg}: The minimum, maximum, and average rotational speeds of the output shaft (half-shaft b), respectively;

- Ripple: The peak-to-peak velocity fluctuation (the difference between f_{max} and f_{min}) of the output shaft.

This dataset represents purely mechanical behavior. The primary goal is to synthesize an RLC equivalent circuit that accurately approximates these kinematic patterns. The complete reference dataset consists of 1,000 states (rows of data), which will be used to validate the precision of the electrical model.

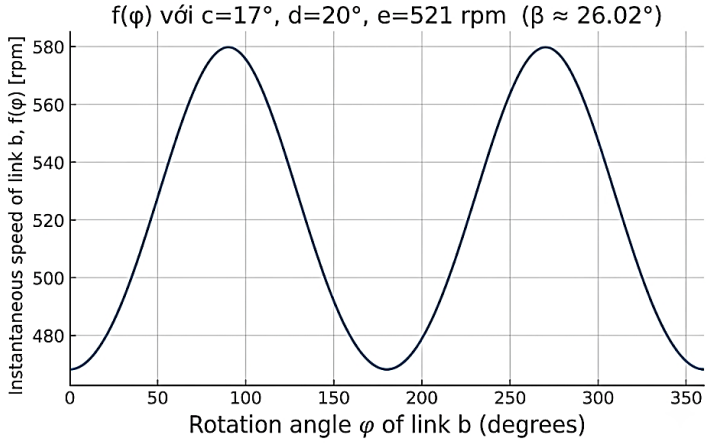


Figure 6. *Output speed fluctuation (f) within a single cycle.*

	A	B	C	D	E	F	G	H
1	c_deg	d_deg	e_rpm	beta_deg	f_min_rpr	f_max_rpr	f_avg_rpm	ripple_pp
2	-30	-30	0	41.40962	0	0	0	0
3	-30	-30	33.33333	41.40962	25	44.44444	33.33333	58.33333
4	-30	-30	66.66667	41.40962	50	88.88889	66.66667	58.33333
5	-30	-30	100	41.40962	75	133.3333	100	58.33333
6	-30	-30	133.3333	41.40962	100	177.7778	133.3333	58.33333
7	-30	-30	166.6667	41.40962	125	222.2222	166.6667	58.33333
8	-30	-30	200	41.40962	150	266.6667	200	58.33333
9	-30	-30	233.3333	41.40962	175	311.1111	233.3333	58.33333
10	-30	-30	266.6667	41.40962	200	355.5556	266.6667	58.33333
11	-30	-30	300	41.40962	225	400	300	58.33333
12	-30	-24	0	37.70655	0	0	0	0

Figure 7. *Excerpt of the mechanical data for simulation.*

2.2.3. Determination of the equivalent RL circuit

Input Parameter Mapping and Voltage Formulation Mapping input parameters (c, d, e) to equivalent sweep frequencies and defining the input voltage U based on A, B, C:

Velocity-Driven Voltage Mapping

Voltage according to angle c

Voltage according to angle d

$$U(s) = R_0 + (R_1 e + L_1 e^2) + (R_2 ce + L_2 c^2) + (R_3 de + L_3 d^2) + [R_5(cd) + L_5(cde)] + [R_6(ce^2) + L_6(de^2)] + [R_7(c^2 d^2) + L_7(e^3)] + offset \quad (16)$$

Voltage according to cross-interaction c.d

Voltage due to rotational inertia

Voltage due to higher harmonics

To bridge the gap between the mechanical and electrical domains, the mechanical inputs (c, d, e) must be mapped to an equivalent electrical excitation. While these parameters are purely mechanical, the RL circuit requires a voltage input, U(s), acting as a frequency sweep to generate an output current I(s) that replicates the predefined velocity ripple.

The fundamental principle for establishing this mapping is Energy Equivalence. The generalized formula for the excitation voltage is defined as:

U(s) = (Static Component) + (Univariate Dynamic Component)
+ (Cross interaction Component)

The priority of the mapping function depends on the nature of the problem:

- Geometric-driven problems: U prioritizes trigonometric functions and radial parameters;

- Velocity-driven problems: U prioritizes second and third-order velocity functions.

In this specific case, the mapped voltage formula is defined as (16).

In this context, the offset represents the time-invariant and frequency-independent component. It functions as the baseline value (zero-shift) of the system when all primary driving variables are null. The voltage U serves as the excitation source applied to the input circuit; fundamentally, this represents the potential energy or the work input into the system.

As a general principle, U(s) is always a function of the state variables that dictate the system's energy scale. The proposed circuit in Figure 2 is essentially a linear filter composed of constant R and L parameters. To ensure this linear structure can match a nonlinear problem, the nonlinearity must be embedded within the excitation source U(s), as demonstrated in expression (16).

Instead of allowing Column A (c) and Column B (d) to interact naturally, we must proactively introduce interaction terms such as $A \cdot B$ or $A \cdot e^2$ into the expression for U. Fundamentally, U must

be a combination of variables where physical coupling is suspected. If these linkages are absent in U, the RL circuit will fail to replicate the behavior because linear components cannot perform autonomous multiplication of state variables.

Based on Figure 1, after aligning the input and output data fields between the two domains under the condition that the RL circuit structure in Figure 2 is predefined, the circuit parameters are identified as follows:

$$Min\sum_{i=1}^{n}[(\mathrm{O})-\mathrm{I}_s]^2 \tag{17}$$

where the output (O) and the current I_s are calculated according to the schematic in Figure 2.

3. RESULTS AND DISCUSSION

The program execution results demonstrate that the approximate accuracy R^2: 0.9402

Component Parameter List:

- R0: -96.8816;
- Branch 1 (R_1, L_1): 2.376×10^{2}, -9.4282×10^{3};
- Branch 2 (R_2, L_2): -3.4117×10^{2}, 2.1599×10^{1};
- Branch 3 (R_3, L_3): 6.7558×10^{2}, 1.3799×10^{1};
- Cross branch 5 (R_5, L_5): 1.4739×10^{1}, 5.1799×10^{1};
- Cross branch 6 (R_6, L_6): 2.4621×10^{3}, -5.2237×10^{3};
- Cross branch 7 (R_7, L_7): 2.3412×10^{1}, 7.1263×10^{4};
- Offset: 93.6458.

With an accuracy of 0.9402, which is equivalent to the performance of a machine learning function under these conditions, the approximation is proven successful. Whether the component values are positive or negative is of secondary importance; this is because the problem can either be represented by a physical circuit (with positive components) or simply utilize circuit principles as a neural framework to leverage its inherent physical significance.

4. CONCLUSIONS

This research has successfully proposed and implemented a novel methodology for approximating the kinematic characteristics of complex mechanical transmissions using an equivalent RL circuit. Based on the results, the following key conclusions can be drawn:

- Approximation performance: The equivalent RL circuit model achieved high precision with an R^2 coefficient of 0.9402. This performance is comparable to traditional machine learning functions, confirming the viability of using electrical structures as surrogate models for mechanical systems.

- Physical interpretability (grey-box modeling**)**: Unlike black-box machine learning models that lack transparency, the proposed method provides a "grey-box" structure with clear physical significance. By leveraging energy equivalence, the circuit parameters (R and L) allow for the explanation of energy flow, dissipation, and inertia within the mechanical domain.

- Nonlinear integration: By proactively embedding nonlinear interactions and state variables into the excitation voltage U(s), the research demonstrated that a linear circuit architecture can effectively replicate highly nonlinear kinematic behaviors, such as the second-order fluctuations of a Cardan joint.

- Research implications: The study aligns with the global trend of Physics-Informed Machine Learning by integrating physical laws into data-driven frameworks. This approach paves the way

for high-speed, circuit-based simulations across diverse engineering domains while maintaining the physical integrity of the original system.

Acknowledgement: *The work presented in this paper is supported by Thai Nguyen University of Technology, Thai Nguyen University, Vietnam.*

REFERENCES

[1]. M. Raissi, P. Perdikaris and G. E. Karniadakis, "*Physics-informed neural networks: A deep learning framework for solving forward and inverse problems involving nonlinear partial differential equations*", Journal of Computational Physics, (2019).
[2]. G. E. Karniadakis, I. G. Kevrekidis, L. Lu, P. Perdikaris, S. Wang and L. Yang, "*Physics-informed machine learning*", Nature Reviews Physics, (2021).
[3]. E. J. Parish and K. Duraisamy, "*A paradigm for data-driven predictive modeling using field inversion and machine learning*", Journal of Computational Physics, (2016).
[4]. A. van der Schaft and D. Jeltsema, "*Port-Hamiltonian system theory: An introductory overview*", Foundations and Trends in Systems and Control, (2014).
[5]. V. H. Nguyen and Q. H. Le, "*Equivalent circuit modeling of parallel robots for energy consumption estimation*", Mechatronics, (2025).
[6]. M. C. Smith, "*The inerter concept and its Foster realization in vehicle suspensions*", Annual Reviews in Control, (2021).
[7]. W. Abbeloos et al., "*Digital twins for parallel robots: Integrating Jacobian maps with real-time physics engines*", Robotics and Computer-Integrated Manufacturing, (2024).
[8]. Y. Sun and Y. Zhao, "*Deep learning vs. analytical models in predicting singularity-free workspaces*", IEEE Robotics and Automation Letters, (2023).
[9]. H. Chen et al., "*Physics-informed neural networks (PINN) for robot kinematics: A hybrid approach*", Nature Machine Intelligence, (2026).
[10]. B. Siciliano and O. Khatib (Eds.), "*Springer Handbook of Robotics*", 3rd ed., Springer, (2024).
[11]. S. Zhu et al., "*Fault diagnosis of parallel robots using impedance fingerprinting*", IEEE Transactions on Industrial Electronics, (2025).
[12]. K. Guo et al., "*Energy-optimal trajectory planning of parallel robots based on equivalent mechanical impedance*", Control Engineering Practice, (2026).
[13]. Le Huu Hung et al., *"Measuring the global and directed propagation of several quality indicators in the optimal design of parallel robots through the evaluation of Lipschitz and GTI indices",* Journal of Military Science and Technology, vol. 112, pp. 11–19, (2026). DOI: 10.54939/1859-1043.j.mst.112.2026.11-19.

TÓM TẮT

Mô phỏng truyền động đẳng tốc không gian bằng mạch xấp xỉ RL tương đương

Trong kỹ thuật nói chung có rất nhiều nghiên cứu không thể hoặc chi phí rất cao để tiếp cận mô hình gốc. Trong các trường hợp đó mô hình gốc có thể được thay thế bằng mô hình tương tự. Tiếp cận này cần có cơ sở toán học chắc chắn để các kết luận dựa trên mô hình tương tự phải đúng với mô hình gốc. Ở góc độ mô hình hoá thuần tuý, mô hình học máy có khả năng xấp xỉ hoá các quy luật rất phức tạp với độ chính xác cao nhưng nó lại không có khả năng giải thích các cơ chế vật lý diễn ra bên trong hiệu ứng đó, vì vậy các mô hình này được coi là hộp đen. Xu hướng mới nhất về học máy trên thế giới là dùng các quan hệ vật lý huấn luyện học máy, điều này có hai lợi ích là độ chính xác vốn là lợi thế dựa trên dữ liệu lớn của học máy và tính giải thích của mô hình vật lý. Bài báo này trình bày các cơ sở toán học để xấp xỉ một atlas động học của một đối tượng cơ học với một mạch RL là đối tượng thay thế trên cơ sở mô hình tương tự của nó. Việc thay thế đạt được độ chính xác cao cho phép mở ra hướng thay thế mọi Atlas bằng mạch điện, mở ra con đường nghiên cứu mô phỏng dựa trên mạch điện cho các đối tượng khác nhau kết hợp được cả độ chính xác và tính minh bạch của hộp xám thay vì hộp đen là hướng nghiên cứu có tiềm năng lớn trong kỹ thuật.

Từ khoá: Học máy; Mô hình hộp đen; Hàm truyền vật lý; Mạch RLC; Bản đồ động học; Cardan.